

HOBET: Connecting LQCD to Nuclear Structure

Kenneth S. McElvain



Berkeley
UNIVERSITY OF CALIFORNIA

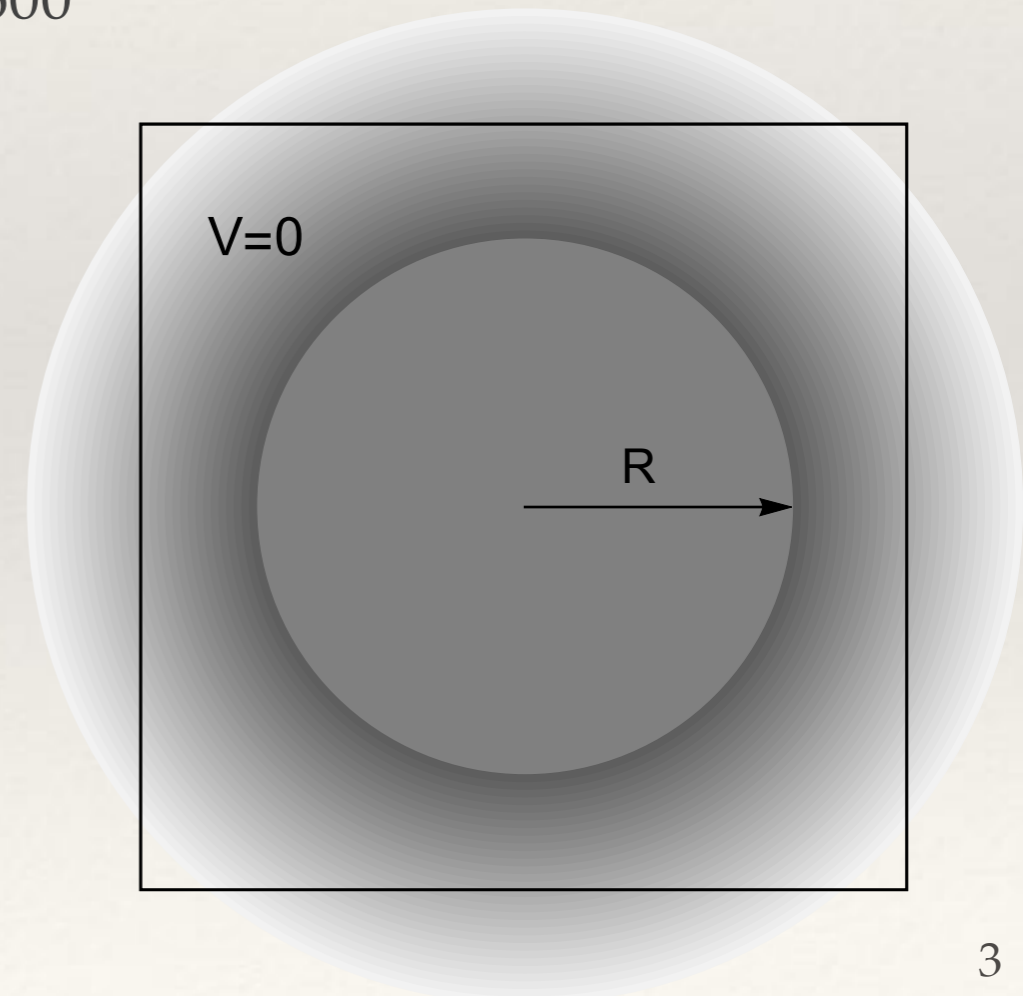


Outline

- ❖ **Part 1:** Construction of the HOBET (Harmonic Oscillator based Effective Theory) interaction from observables in spherical infinite volume form.
- ❖ **Part 2:** Construction of the HOBET interaction in Cartesian form from the spectrum in a periodic box.
- ❖ The magic trick is that the LECs of the two forms can be related.

Interactions from LQCD

- ❖ Lüscher's method can be used to map the spectrum to phase shifts.
 - ❖ Use traditional path: collect enough phase shift data in multiple channels and use to fit an effective theory or a model like a realistic potential.
- ❖ HAL QCD potential method, Doi *et al.* arXiv:1702.01600
 - ❖ Construct Nambu-Bethe-Salpeter wave function and infer non-local potential.
- ❖ Sources of error
 - ❖ Both: Tail of interaction exceeding $L/2$.
 - ❖ Lüscher's method: Divergences of zeta function in higher order terms.
 - ❖ HAL QCD potential: non-elastic excited state contamination.



Nuclear Structure Calculations

- ❖ Configuration interaction calculations use an explicitly anti-symmetric basis of Slater determinants over a single particle basis.
- ❖ While the basis size grows very fast with the size of the single particle basis and A , the number of particles, fantastically efficient matrix techniques can be used to find the low lying spectrum.
- ❖ The required calculation cutoff on the basis ignores scattering through excluded states. This requires an *effective* interaction constructed in the HO basis that takes such scattering into account.

The Bloch-Horowitz Equation

P is projection operator to space to work in, $Q = 1 - P$

$$H_{\text{eff}}(E_i)|\psi_i\rangle = P\left(H + H\frac{1}{E_i - QH}QH\right)P|\psi_i\rangle = E_i P|\psi_i\rangle$$

- ❖ Eigenstates of $H_{\text{eff}}(E)$ are projections with the same eigenvalues.
 - ❖ All eigenstates that overlap P are included!
- ❖ Eigenstates are not orthogonal.
- ❖ Explicitly energy dependent: Must solve self consistently.
- ❖ Operators are formally renormalized as:

$$\hat{O}_{\text{eff}}(E) = \frac{E}{E - HQ} \hat{O} \frac{E}{E - QH}$$

ET and The HO Basis

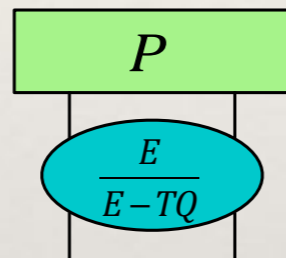
- ❖ In a typical EFT using a momentum basis T is diagonal and does not couple P & Q .
- ❖ In the HO basis T is a hopping operator, strongly connecting the last P state to the lowest Q state.
 - ❖ Bad news for an ET expansion.
 - ❖ Maybe H_{eff} can be reorganized, isolating T ...

The Effective Theory Expansion

The Haxton-Luu form of the Bloch-Horowitz Equation

$$H_{eff}(E) = P \frac{E}{E - TQ} \left[T + T \frac{Q}{E} T + V + \underbrace{V \frac{1}{E - QH} QV}_{V_{IR} + V_{\delta}} \right] \frac{E}{E - QT} P$$

$V_{IR} + V_{\delta}$ *ET Substitution*

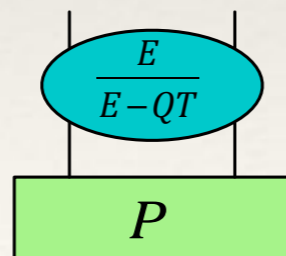
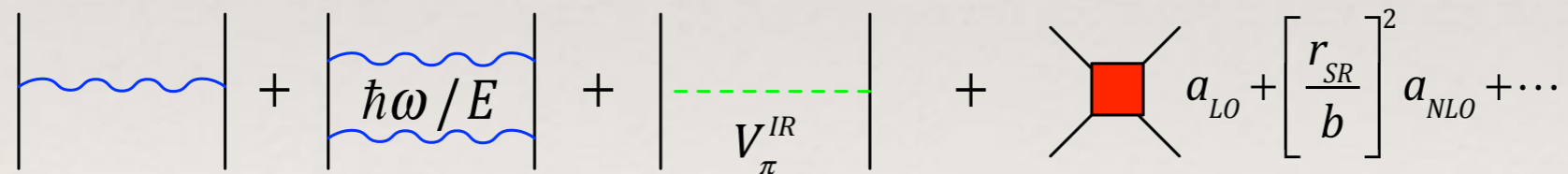


Far INFRA-RED

Far INFRA-RED

Regulated, NEAR IR

UV



Far INFRA-RED

Green's Function for $E/(E-QT)$

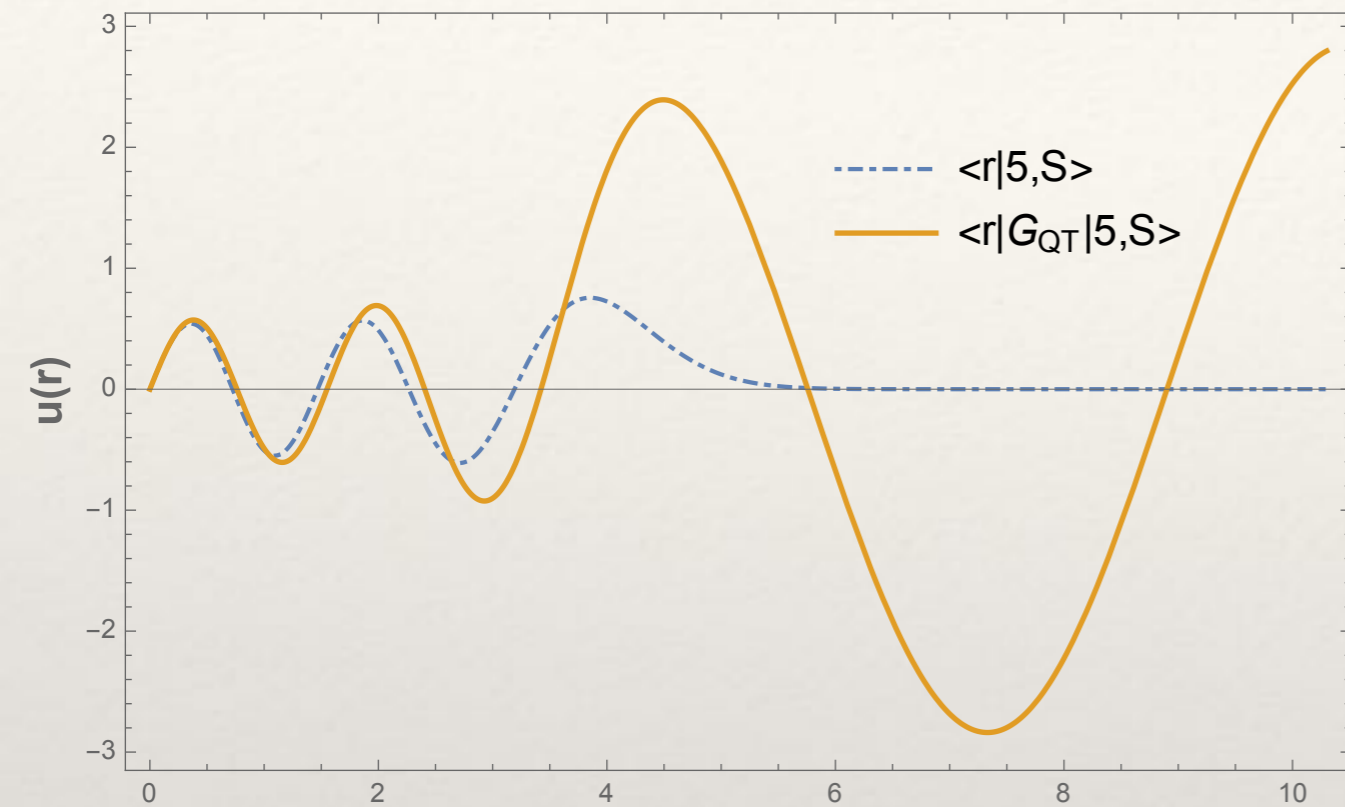
- ❖ Simplify: $|\tilde{i}\rangle = \frac{E}{E-QT}|i\rangle = b_{ij} \frac{E}{E-T}|j\rangle$, $b_{ij} = \left\{ P \frac{E}{E-T} P \right\}_{ij}^{-1}$, $i, j \in P$
- ❖ GF for $E/(E-T)$ is expressed in terms of solutions of $(E-T)u=0$

$$u_{in}(r) = kr j_\ell(kr), \quad u_{out}(r) = kr \left(-\cot(\delta_\ell) j_\ell(kr) + \eta_\ell(kr) \right)$$

$$g(r, r') \propto \begin{cases} u_{in}(r)u_{out}(r') & r < r' \\ u_{out}(r)u_{in}(r') & r > r' \end{cases}$$

- ❖ For $r > \text{range}(\text{HO basis})$ the form of the transformed edge state is $u_{out}(r)$.
- ❖ The boundary condition at infinity is specified by δ_ℓ .

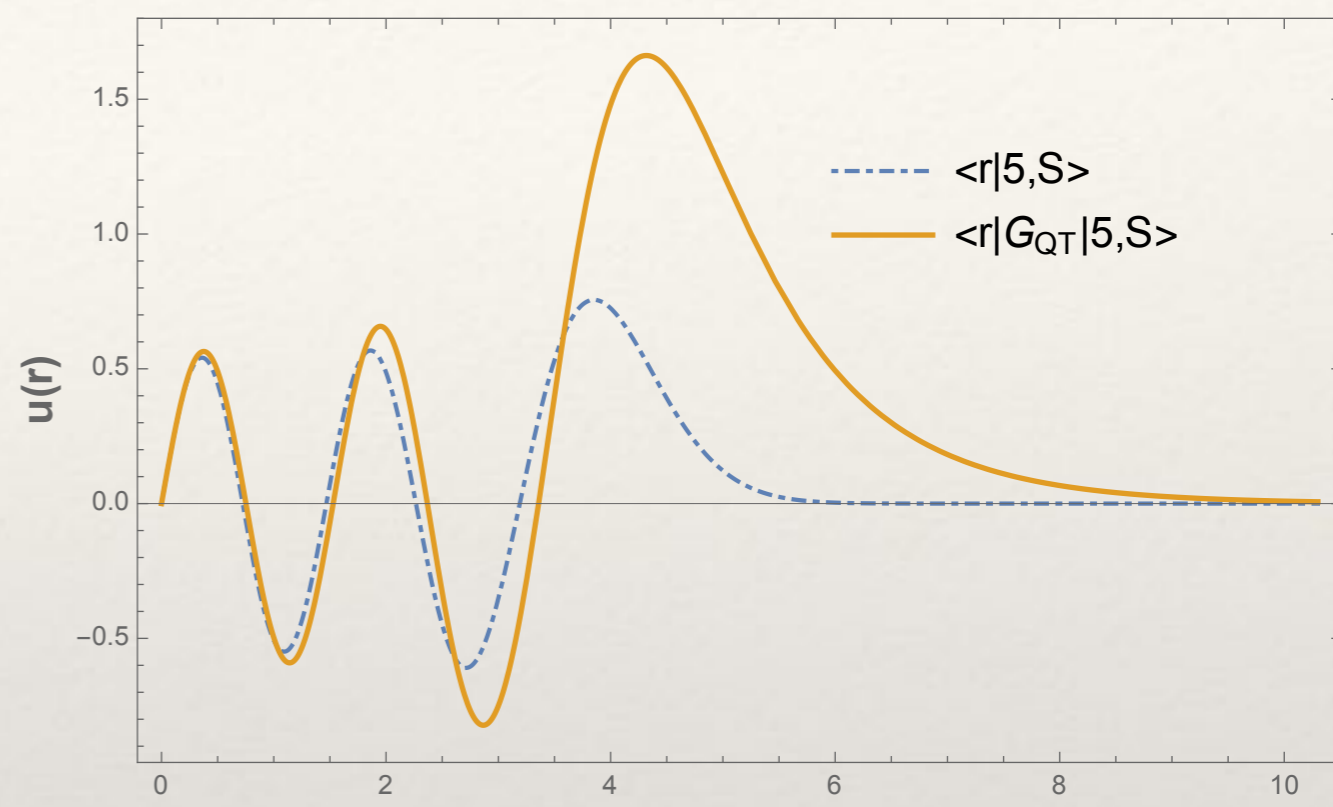
Transform of Edge States



- ❖ Acting on edge state with $E/\hbar\omega = 1/2$.

Recovers scattering wave function with phase shift.

- ❖ $E/(E-QT)$ with boundary condition recovers IR behavior.



- ❖ Acting on edge state with $E/\hbar\omega = -1/2$.

Recovers bound state exponential decay from gaussian falloff of HO state.

Sum T to All Orders

- ❖ T contributions can be summed to all orders.

$$\left\langle j \left| \frac{E}{E - TQ} \left[T + T \frac{Q}{E} T \right] \frac{E}{E - QT} \right| i \right\rangle = E \left(\delta_{ji} - b_{ji} \right)$$

$$b_{ij} = \left\{ P \frac{E}{E - T} P \right\}_{ij}^{-1}$$

- ❖ A surprisingly simple result.
- ❖ A non-perturbative sum of kinetic energy scattering is key to a convergent ET expansion of the remaining parts.

The Operator Expansion

- ❖ Described in terms of HO lowering operators.

$$\hat{c} \text{ lowers } L, \hat{a} \text{ lowers nodal } n, \quad [\hat{c}, \hat{a}] = 0$$

$$V_{\delta}^S = a_{LO}^S \delta(r) + a_{NLO}^S (\hat{a}^{\dagger} \delta(r) + \delta(r) \hat{a}) + \dots$$

$$V_{\delta}^{SD} = a_{NLO}^{SD} (\hat{c}^{\dagger 2} \delta(r) + \delta(r) \hat{c}^2) + a_{NNLO}^{22,SD} (\hat{c}^{\dagger 2} \delta(r) \hat{a} + \hat{a}^{\dagger} \delta(r) \hat{c}^2) \\ + a_{NNLO}^{40,SD} (\hat{c}^{\dagger 2} \hat{a}^{\dagger} \delta(r) + \delta(r) \hat{a} \hat{c}^2) + \dots$$

- ❖ This is slightly simplified by absorbing a constant related to coupling spins to angular momentum into the LECs.

Matrix Structure: $^1S_0, \Lambda=8$

$$\langle \tilde{j} | V_\delta | \tilde{i} \rangle^S = a_{LO}^S \pi^{-3/2} \begin{bmatrix} 1 & \sqrt{3/2} & \sqrt{15/8} & \sqrt{35/16} & \mathbf{0.947} \\ \sqrt{3/2} & 3/2 & \sqrt{45/16} & \sqrt{105/64} & \mathbf{1.160} \\ \sqrt{15/8} & \sqrt{45/16} & 15/8 & \sqrt{105/128} & \mathbf{1.297} \\ \sqrt{35/16} & \sqrt{105/64} & \sqrt{105/128} & 35/16 & \mathbf{1.401} \\ \mathbf{0.947} & \mathbf{1.160} & \mathbf{1.297} & \mathbf{1.401} & \mathbf{0.898} \end{bmatrix}$$

- ❖ Edge state matrix elements in **red** vary with E due to Green's function action on edge states.
- ❖ Each such matrix corresponds to a pair (E_i, Bdy_i) .

Fitting LECs

- ❖ Principle: The BH equation is energy self consistent

$$H_{eff}^{full} P|\psi_i\rangle = E_i P|\psi_i\rangle$$

- ❖ At fixed order we have a nearby eigenstate.

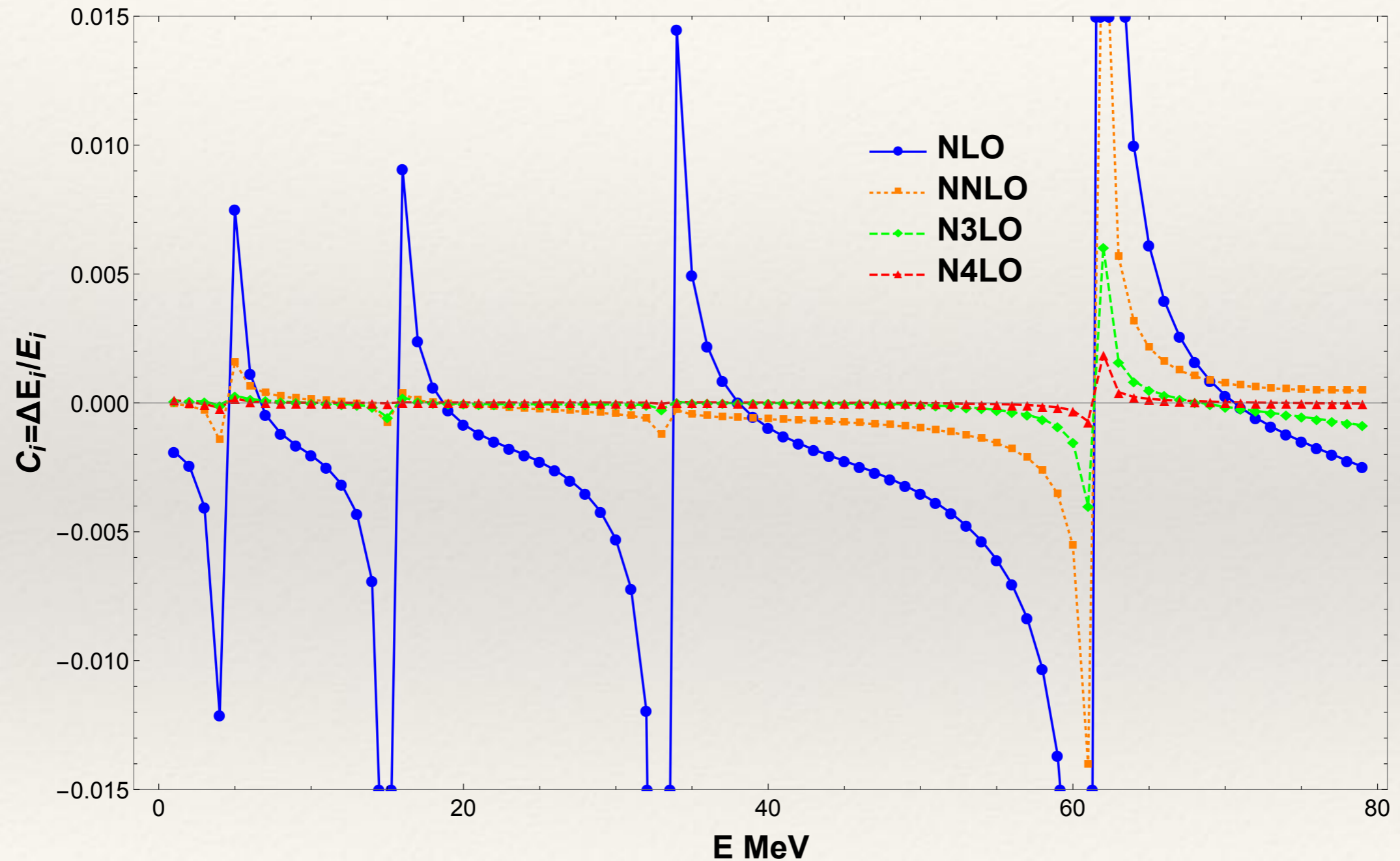
$$H_{eff}(LECs) P|\psi'_i\rangle = \varepsilon_i P|\psi'_i\rangle$$

- ❖ The mismatch must be due to LEC values.

- ❖ Repair by minimizing $\sum_{i \in \text{samples}} W(i) (\varepsilon_i - E_i)^2 / \sigma_i^2$

- ❖ The variance can be replaced by a full covariance matrix.

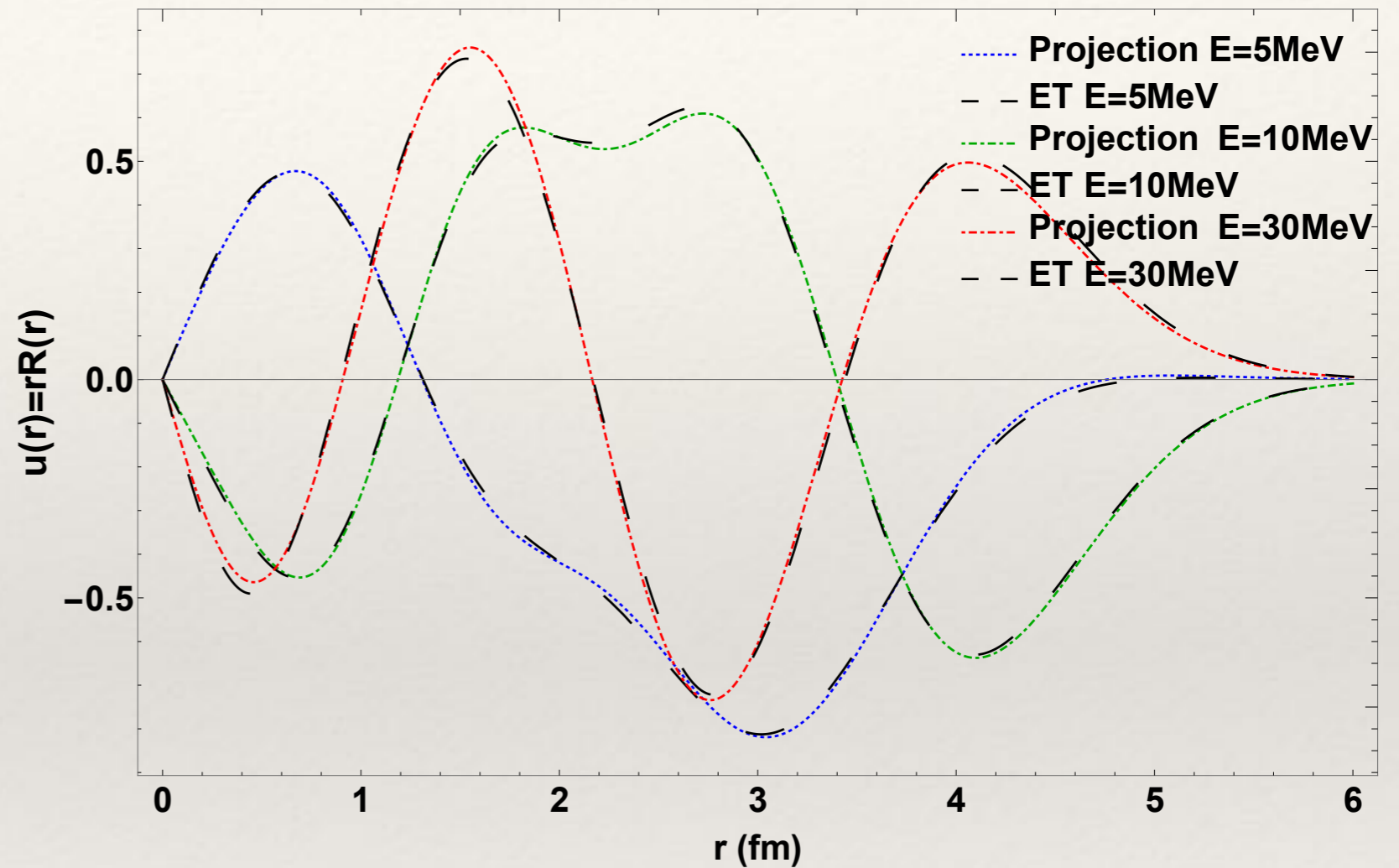
S-Channel Eigenvalue Convergence



Test potential : hard core + well

P Channel Wave Function

- ❖ ET Wave functions should match projections of numerical solutions.



- ❖ Colored lines are the projections of numerical solutions. Black dashed lines are the effective theory solutions at the same energies.

Part 1 Conclusions

- ❖ The HOBET interaction can be directly constructed from observables such as phase shifts in the continuum
- ❖ LQCD can produce nuclear phase shifts, subject to statistical errors and uncorrected finite volume effects.
- ❖ In combination, a nuclear effective interaction is produced that can be used in A -body calculations.

Outline

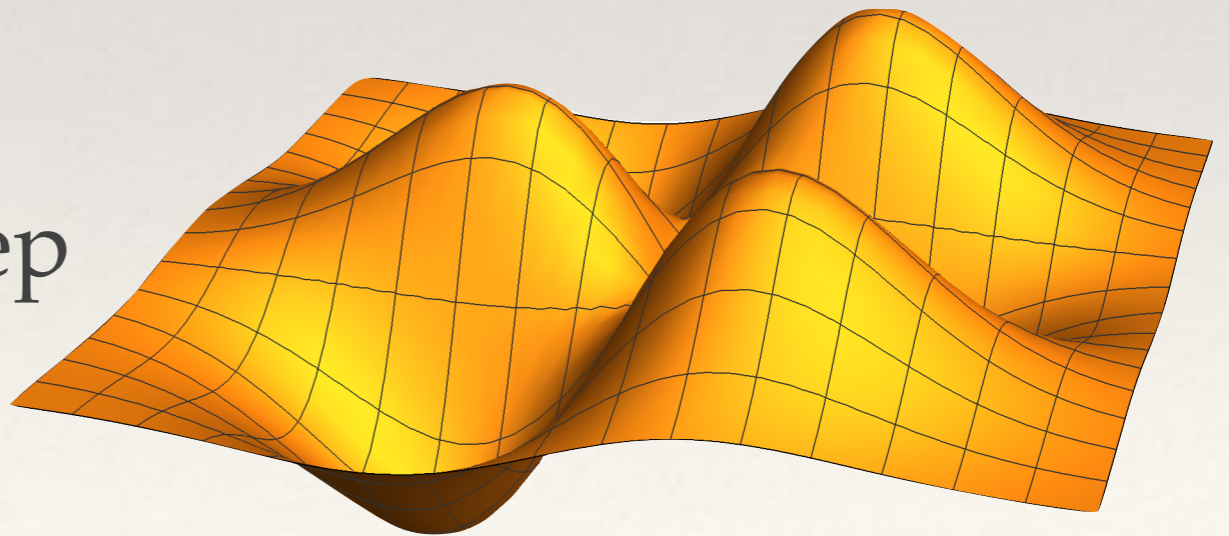
- ❖ Part 1: Construction of the HOBET (Harmonic Oscillator based Effective Theory) interaction from observables in spherical infinite volume form.
- ❖ Part 2: Construction of the HOBET interaction in Cartesian form from the spectrum in a periodic box.
 - ❖ The magic trick is that the LECs of the two forms can be related.

Boundary Conditions

- ❖ Phase shifts as boundary conditions are replaced by periodic boundary conditions.
- ❖ Small volumes limit the number of states in energy range of interest.
- ❖ ET construction should support
 - ❖ Multiple volumes to access more states.
 - ❖ Boosting

Cartesian Harmonic Oscillator

- ❖ 3D harmonic oscillator can be equivalently represented in spherical or Cartesian form.
- ❖ Brackets $\langle n_x n_y n_z | n \ell m \rangle$ relate states in each energy level.
- ❖ Quanta based cutoff is consistent - key
- ❖ The Cartesian form will be convenient for the periodic boundary conditions.
- ❖ Pick HO length scale to keep the basis away from edges in all volumes.



Periodic Momentum Basis

- ❖ Even and odd basis functions
- ❖ m ranges from $-N/2$ to $N/2$ with $m < 0$ indicating *sin* basis functions
- ❖ The kinetic energy operator is a bit complicated by the varying side lengths:

$$\phi_{i,s,m}(x) = \sqrt{2/L_i} \sin(\alpha_{i,m}x), \quad m = 1, \dots, N/2$$

$$\phi_{i,c,0}(x) = \sqrt{2/L_i} (1/\sqrt{2}), \quad m = 0$$

$$\phi_{i,c,m}(x) = \sqrt{2/L_i} \cos(\alpha_{i,m}x), \quad m = 1, \dots, N/2$$

$$\text{with } \alpha_{i,m_i} = 2\pi|m_i|/L_i$$

$$\phi_{\vec{m}}(x, y, z) = \phi_{m_x}(x) \phi_{m_y}(y) \phi_{m_z}(z)$$

$$\begin{aligned} \hat{T} \phi_{\vec{m}}(x, y, z) &= 2\pi^2 \left(\sum_i \frac{m_i^2}{L_i^2} \right) \phi_{\vec{m}} \\ &= \lambda_{\vec{m}} \phi_{\vec{m}}(x, y, z) \end{aligned}$$

Green's Function for $E/(E-QT)$

- ❖ As before: $|\tilde{i}\rangle = \frac{E}{E-QT}|i\rangle = b_{ij} \frac{E}{E-T}|j\rangle$, $b_{ij} = \left\{ P \frac{E}{E-T} P \right\}_{ij}^{-1}$, $i, j \in P$
- ❖ $E/(E-T)$ is expressed as a bilinear eigenfunction expansion over the periodic basis functions.

$$G_T(E; \mathbf{r}, \mathbf{r}') = \sum_{\vec{m}} \frac{E}{E - \lambda_{\vec{m}} + i\epsilon} \phi_{\vec{m}}(\mathbf{r}) \phi_{\vec{m}}(\mathbf{r}')$$

$$b_{\vec{n}'\vec{n}} = \langle \vec{n}' | G_T | \vec{n} \rangle = \sum_{\vec{m}} \frac{E}{E - \lambda_{\vec{m}}} \langle \vec{n}' | \phi_{\vec{m}}(\vec{r}') \phi_{\vec{m}}(\vec{r}) | \vec{n} \rangle = \sum_{\vec{m}} \frac{E}{E - \lambda_{\vec{m}}} \chi_{\vec{n}'\vec{m}} \chi_{\vec{n}\vec{m}}$$

where $\chi_{\vec{n},\vec{m}} = \chi_{n_x,m_x} \chi_{n_y,m_y} \chi_{n_z,m_z}$, $\chi_{n,m} = \int_{-\infty}^{\infty} dx H_n(x) \phi_m(x)$

3D basis overlap
Calculated on the fly

1D basis overlap
Stored

Evaluate by Inserting Periodic Basis

Sum T to all orders:
$$\left\langle \vec{n}' \left| \frac{E}{E-TQ} \left[T + T \frac{Q}{E} T \right] \frac{E}{E-QT} P \right| \vec{n} \right\rangle = E(\delta_{\vec{n}'\vec{n}} - b_{\vec{n}'\vec{n}})$$

- ❖ V_{IR} matrix elements are the most expensive part of H_{eff}

$$\left\langle \vec{n}' \left| G_{TQ} V_{IR} G_{QT} \right| \vec{n} \right\rangle = \sum_{\vec{m}', \vec{m}, \vec{s}, \vec{t}} b_{\vec{n}', \vec{s}} \frac{E}{E - \lambda_{\vec{m}'}} \langle \vec{s} | \vec{m}' \rangle \langle \vec{m}' | V_{IR} | \vec{m} \rangle \langle \vec{m} | \vec{t} \rangle \frac{E}{E - \lambda_{\vec{m}}} b_{\vec{t}, \vec{n}}$$

- ❖ All pieces are precomputed, but sum is still very large.
- ❖ For $\vec{n}', \vec{n} \in P^-$ $G_{QT}=1$, which can be used to check results.

Magic with V_δ

- ❖ As long as V_δ on P^- doesn't interact with the boundary it is the same object in both finite and infinite volume contexts.
- ❖ Spherical and Cartesian HO bases are simply representations related by brackets.

- ❖ Cartesian ET expansion respecting parity invariance.

Table 9.1: LECs and Cartesian operators

| LEC | operators |
|------------|---|
| $c000d000$ | $\delta(r)$ |
| $c100d100$ | $(a_x^\dagger \delta(r) a_x + a_y^\dagger \delta(r) a_y + a_z^\dagger \delta(r) a_z)$ |
| $c100d010$ | $(a_x^\dagger \delta(r) a_y + a_x^\dagger \delta(r) a_z + a_y^\dagger \delta(r) a_z) + \text{h.c.}$ |
| $c200d000$ | $(a_x^{\dagger 2} + a_y^{\dagger 2} + a_z^{\dagger 2}) \delta(r) + \text{h.c.}$ |
| $c110d000$ | $(a_x^\dagger a_y^\dagger + a_x^\dagger a_z^\dagger + a_y^\dagger a_z^\dagger) \delta(r) + \text{h.c.}$ |

Relating Spherical to Cartesian V_δ

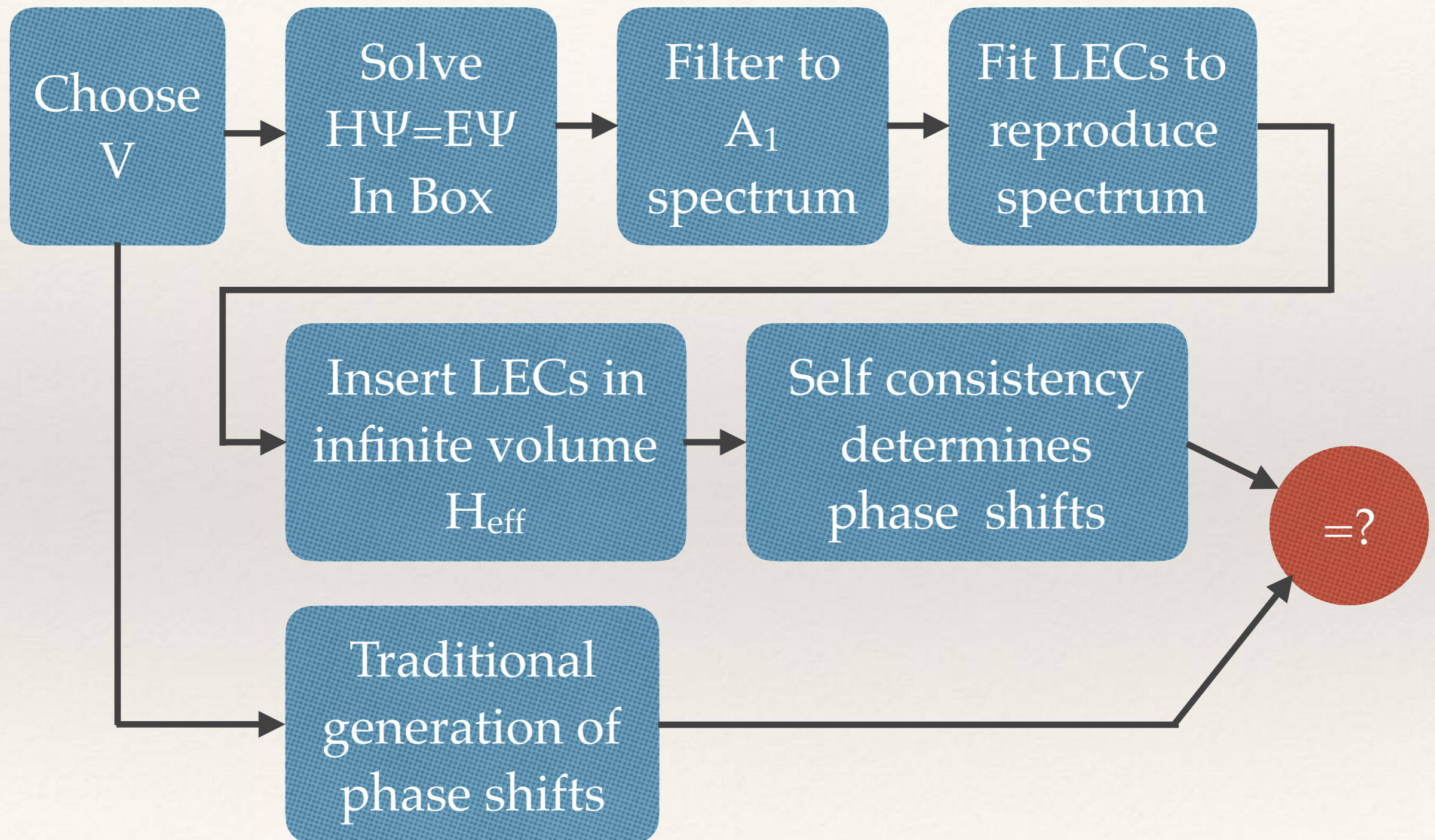
- ❖ Symmetries:
 - ❖ Cartesian construction: parity invariance.
 - ❖ Spherical construction: parity and rotational invariance.
- ❖ Setting $V_{\delta, cart} = V_{\delta, sph}$ on P^- imposes rotational invariance.
- ❖ Cartesian LECs are replaced by linear comb of spherical LECs, including in edge state matrix elements.

Example:

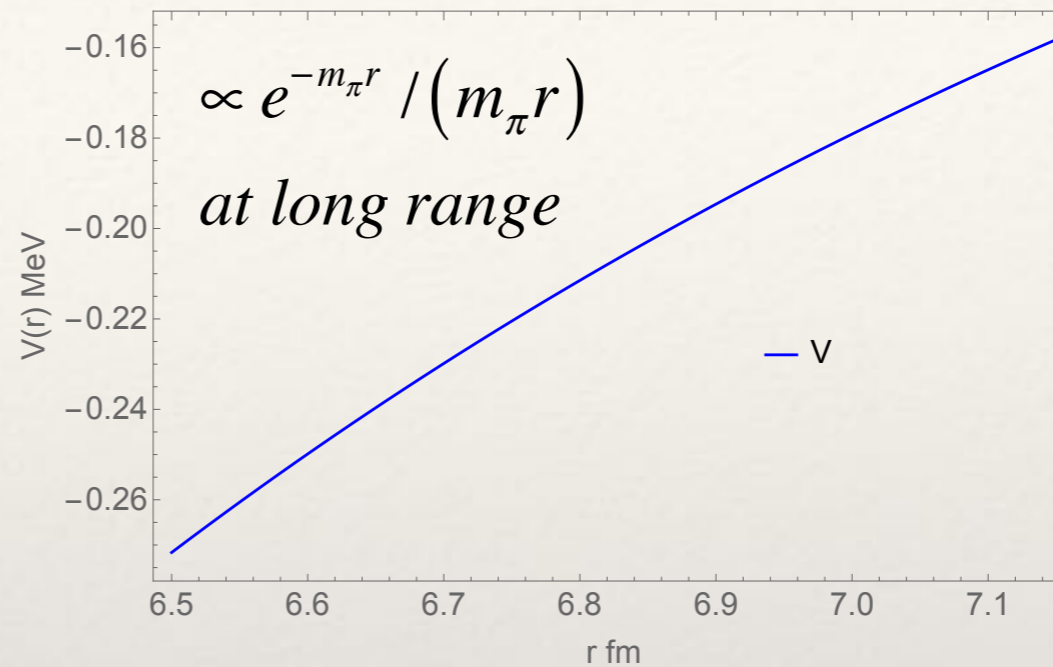
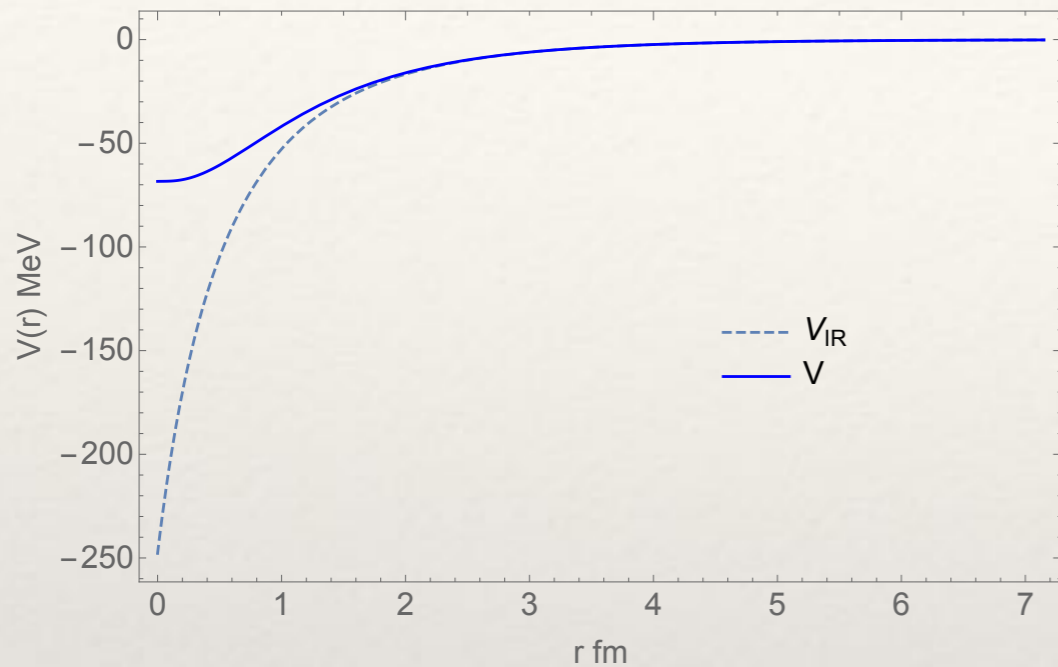
$$c_{200}d_{200} = a_{NNLO22}^{1S0} + (2/3)a_{NNLO}^{1D2}$$

$$c_{200}d_{020} = a_{NNLO22}^{1S0} - (1/3)a_{NNLO}^{1D2}$$

Testing Plan



Test Setup: $\text{Range}(V) > L/2$



$$L = 14.3 \text{ fm}$$

$$m_{\pi}L = 10$$

- ❖ Periodic images of the potential make a contribution.
- ❖ Infinite volume bound state at -4.05 MeV.
- ❖ LECs are fit using states with $L=0$ overlap.

| Rep | MeV | L=0 | L=2 | L=4 | L=6 |
|---------|---------|-------|-------|-------|-------|
| A_1^+ | -4.4428 | 0.5 | 0 | 0.866 | 0 |
| A_1^+ | 2.0314 | 0.155 | 0 | 0.988 | 0 |
| E^+ | 7.5995 | 0 | 0.424 | 0.361 | 0.830 |
| E^+ | 15.2980 | 0 | 0.474 | 0.393 | 0.788 |
| A_1^+ | 21.6167 | 0.326 | 0 | 0.265 | 0.908 |
| E^+ | 23.2423 | 0 | 0.468 | 0.597 | 0.651 |
| A_1^+ | 29.4041 | 0.521 | 0 | 0.853 | 0.023 |
| E^+ | 30.9457 | 0 | 0.567 | 0.428 | 0.704 |
| A_1^+ | 35.2449 | 0.655 | 0 | 0.189 | 0.732 |
| E^+ | 38.4043 | 0 | 0.882 | 0.176 | 0.437 |
| A_1^+ | 45.1402 | 0.526 | 0 | 0.576 | 0.625 |

Phase Shift Setup

- ❖ Reference phase shifts for $L=0$ and $L=4$ are directly calculated from V .
- ❖ HOBET S-channel phase shifts are computed from the N3LO LECs that reproduce the spectrum. The phase shift is found by dialing the phase shift to produce energy self consistency.
- ❖ Lüscher's method phase shifts come from the formula
$$k \cot \delta_0 = \frac{2}{\sqrt{\pi L}} \mathcal{Z}_{0,0}(1; \tilde{k}^2) + \frac{12288\pi^7}{7L^{10}} \frac{\mathcal{Z}_{4,0}(1; \tilde{k}^2)^2}{k^9 \cot \delta_4} + \mathcal{O}(\tan^2 \delta_4)$$
Luu, Savage,
arXiv:1101.3347
- ❖ An effective range expansion up to k^6 is used to interpolate.
- ❖ For simplicity the second term is evaluated using the $L=4$ phase shift directly determined from V .

Phase Shift Results

$$L = 14.3 \text{ fm}$$

$$m_\pi L = 10$$

The V column should be considered the reference.

| E MeV | V | HOBET | Leading Lüscher | Next Order Lüscher |
|-------|---------|---------|-----------------|--------------------|
| 1 | 142.023 | 141.931 | 142.552 | 142.751 |
| 2 | 128.972 | 128.860 | 129.571 | 129.823 |
| 4 | 113.602 | 113.464 | 114.205 | 114.403 |
| 8 | 96.919 | 96.752 | 97.575 | 97.3135 |
| 10 | 91.473 | 91.296 | 92.228 | 91.6403 |
| 15 | 81.672 | 81.480 | 82.852 | 81.3184 |
| 20 | 74.876 | 74.691 | 76.667 | 74.0936 |

- ❖ A potential source of error for both HOBET and Lüscher's method is the accuracy of the finite volume spectrum.
- ❖ Solved three times with $N=350,400,450$ and made a continuum extrapolation. The 3 results showed a consistent and small evolution of the eigenvalues.

Observations on Errors

- ❖ Images double the potential contribution at the center of the faces.
- ❖ For HOBET the impact is suppressed by two powers of V in $V(1/(E - QH))QV$.
- ❖ The second order correction for Lüscher's method is significant. In this trial parts of the spectrum fell near the divergences of $\mathcal{Z}_{4,0}$.

New Idea - Better Isolation

$$V = V_{UV} + V_{IR} \quad \text{e.g. } V_{UV} - \text{unknown, } V_{IR} = \text{OPEP}$$

$$\begin{aligned} V \frac{1}{E - QH} QV &= (V_{UV} + V_{IR}) \frac{1}{E - QT - QV_{IR} - QV_{UV}} Q(V_{UV} + V_{IR}) \\ &= V_{IR} \frac{1}{E - QT - QV_{IR}} QV_{IR} + V_{UV} [\dots] + [\dots] V_{UV} \end{aligned}$$

- ❖ This motivates a new ET substitution.

$$V + V \frac{1}{E - QH} QV \rightarrow V_{IR} + V_{IR} \frac{1}{E - QH_{IR}} QV_{IR} + V_{\delta}$$

- ❖ V_{δ} becomes much shorter range, enabling the use of even smaller volumes.

Part 2: Conclusions

- ❖ The Cartesian finite volume HOBET interaction LECs are directly fit to the spectrum in a set of volumes.
- ❖ The same LECs are used in both infinite and finite volume forms.
- ❖ Finite volume effects are isolated from the ET expansion.
 - ❖ Issues common to other methods with the range of V are suppressed.
 - Allows smaller volumes for LQCD calculations.
- ❖ A direct test of both HOBET and Lüscher's method was made.
- ❖ Future: A 3-body interaction can be fit to a 3-body spectrum.

End